COMMUNICATION

A Structurally Characterized Cobalt(I) σ–Alkane Complex

Timothy M. Boyd,[a] Bengt E. Tegner,[b] Graham J. Tizzard,[c] Antonio Martínez–Martínez,[a] Samuel E. Neale,[b] Michael A. Hayward,[a] Simon J. Coles,[b] Stuart A. Macgregor,*[b] Andrew S. Weller.*[a]

Abstract: The synthesis, and single–crystal x-ray structure, of a cobalt σ–alkane complex, [Co(Cy$_2$P(CH$_2$)$_4$PCy$_2$)(norbornane)][BAr$^F_4$], is achieved by a single–crystal to single–crystal solid/gas hydrogenation from a norbornadiene precursor. Magnetic data show this complex to be a triplet. Periodic DFT and electronic structure analyses identify weak C–H→Co σ-interactions, augmented by dispersive stabilisation between the alkane ligand and the anion–microenvironment. The calculations are most consistent with a η^1:η^1-alkane binding mode.

σ–Alkane complexes, where a C–H group interacts with a metal, in a 3–center 2–electron bond (3c–2e), are key intermediates in stoichiometric and catalytic hydrocarbon C–H activation processes.[1, 2] The directional, non–nucleophilic and strong C–H bond means that alkanes are poor ligands (40–60 kJ mol^{-1}), making σ–alkane complexes challenging to observe, due to displacement by solvent or other ligands.[3] Elegant methods have thus been developed to generate and characterize σ–alkane complexes in the solution–phase (Fig. 1A). Low temperature NMR spectroscopy, using in situ photolysis or protonolysis, reveals σ–alkane complexes such as **1**[4] and **2**,[5] respectively, while fast time–resolved spectroscopic studies (TRIR)[6] probe the formation and onward reactivity of transient σ-alkane complexes (e.g. **3**).[7, 8]

We have recently developed molecular solid–state routes to σ–alkane complexes that circumvent the need for solvent. By using single–crystal to single–crystal (SC-SC) gas/solid reactivity[9, 10] synthetically significant amounts (up to ~1 g) of σ–alkane complexes such as **[Rh(L1)–NBA][BAr$^F_4$]** (Fig. 1B, NBA = norbornane, Ar^F = 3,5–(CF$_3$)$_2$C$_6$H$_3$, **L1** = Cy$_2$PCH$_2$CH$_2$PCy$_2$) can be formed by simple hydrogenation of a diene precursor (norbornadiene, NBD). These complexes can show remarkable stabilities (months, 25 ºC),[11] allowing for their full characterization (single–crystal x-ray diffraction, solid–state NMR) and studies into alkane mobility and reactivity.[10, 12, 13] Their isolation comes, in large part, from the stabilizing [BAr$^F_4$]$^-$ anion microenvironment which often forms an ~O_h cage surrounding the metal cation. We

[a] T. M. Boyd, Dr A. Martínez–Martínez, Prof. M. Hayward, Prof. A. Weller
Chemistry Research Laboratories, Department of Chemistry, University of Oxford, Oxford OX1 3TA (UK)
E-mail: andrew.weller@chem.ox.ac.uk
[b] Dr B. Tegner, S. Neale, Prof. S. Macgregor
Institute of Chemical Sciences, Heriot-Watt University, Edinburgh EH14 4AS (UK)
E-mail: S.A.Macgregor@hw.ac.uk
[c] Dr G. Tizzard, Prof. S. Coles
UK National Crystallography Service, Chemistry, Faculty of Natural and Environmental Sciences, University of Southampton, Southampton SO17 1BJ (UK)

Supporting information and the ORCID identification number(s) for the author(s) of this article can be found under:

have termed this methodology Solid–state Molecular OrganoMetallic (SMOM) chemistry.[12]
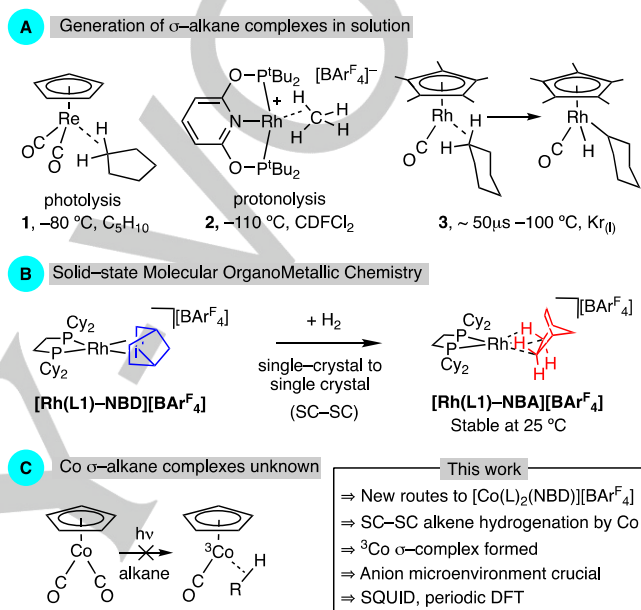

Figure 1. (A) Examples of σ-alkane complexes, generated using in situ photolysis (**1**) or protonation (**2**), and as intermediates in C–H activation (**3**). (B) Single–crystal to single–crystal generation of a Rh σ–alkane complex by hydrogenation of a diene. (C) Instability of Co σ–alkane complexes.

Despite these advances in both solution and solid-state chemistries there remain significant challenges. One of these is that while the heavier congeners of group 9 (Rh and Ir) have offered a rich hunting ground for the generation of σ–alkane complexes and subsequent catalytic C–H activation,[2, 3, 7, 14] no cobalt examples are known. Indeed the only σ–alkane complex of cobalt so far reported in the literature is Co(CH$_4$), generated using isolated Co atoms in an Ar matrix at –261 ºC.[15] While the 3d–metal cobalt is expected to form weak 3c–2e bonds with alkanes, an additional problem is the accessibility of the ^{3}Co–spin state, that further discourages the formation of strong bonds. For example, while the photogenerated {^{1}Rh(CO)Cp*} fragment forms a transient σ–alkane complex (**3**),[7] no such complexes are observed for equivalent {^{3}Co(CO)Cp} (Fig. 1C).[16] Calculations show that a ^{3}Co(CO)Cp···HCH$_3$ interaction would be repulsive, and while ^{1}Co(CO)Cp···HCH$_3$ is accessible, its formation is endergonic with respect to the reactants.[17] In contrast, σ–H$_2$ complexes of cobalt are known.[18] A related species ^{3}Mn(CO)$_3$Cp(heptane) is characterized indirectly, using TRIR and kinetic modeling, and is a very short lived species.[19]

We now report that, by harnessing the stabilizing microenvironment of the [BAr$^F_4$]$^-$ anions and a suitability designed

Co–NBD precursor, we have been able to structurally characterize a very weakly–bound Co σ–alkane complex using SMOM–techniques. This also has a ^{3}Co spin state – as probed by magnetic measurements and computation.

[Rh(L)–NBD][BAr$^F_4$] is a versatile motif for the generation of σ–alkane complexes by SC–SC transformations (L = Cy$_2$P(CH$_2$)$_n$PCy$_2$).[9, 11] We have thus developed a route to the equivalent cobalt(I) complexes of these Schrock–Osborne[20] systems (Fig. 2; n = 2, **L1**; n = 4, **L2**). This starts from CoCl$_2$, involves a KC$_8$ reduction, a CH$_2$Cl$_2$ extraction, and delivers, respectively, lilac and green crystalline products in moderate yield.[21] Our method complements that recently reported by Chirik using DuPhos–based ligands.[22] [Co(L1)(arene)][BF$_4$] complexes are also known.[23] The solid–state structure of **[Co(L2)–NBD][BAr$^F_4$]** is shown in Fig. 2, with that for **[Co(L1)–NBD][BAr$^F_4$]** given in the supporting materials. Both show the cobalt coordination sphere is twisted from square planar towards tetrahedral. This distortion is greater with the wider bite angle ligand in **[Co(L2)–NBD][BAr$^F_4$]** (28.0(3)º versus 22.5(2)º).[24] The [BAr$^F_4$]$^-$ anions adopt the ~O_h motif in the solid–state, being very similar to the direct analogs **[Rh(L)–NBD][BAr$^F_4$]**.[9, 11]
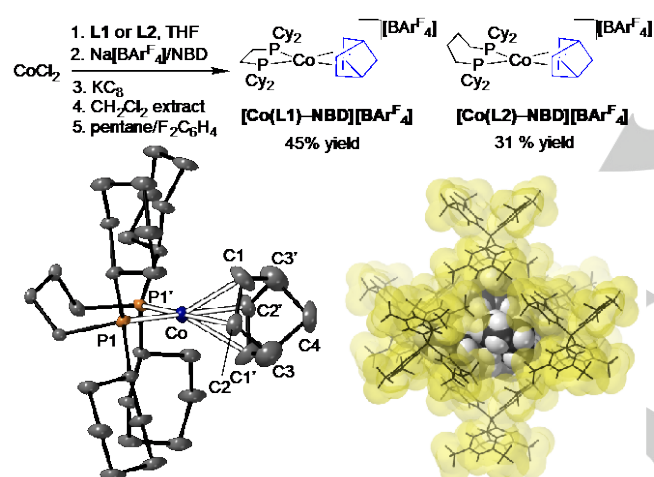
Figure 2. Synthesis of cationic Co–NBD precursors. **L1** = Cy$_2$P(CH$_2$)$_2$PCy$_2$, **L2** = Cy$_2$P(CH$_2$)$_4$PCy$_2$. Solid–state structure of the cationic portion of **[Co(L2)–NBD][BAr$^F_4$]**, 15% displacement ellipsoids, anion and H–atoms not shown, –173 ºC data collection. ~O_h packing of [BAr$^F_4$]$^-$ anions around a single cation. Surfaces shown at van der Waals radii. Selected bond lengths (Å) and angles (º): Co–C1, 2.212(6) Co–C2, 2.110(4); C1–C2, 1.394(6); Co–P1, 2.2717(8); P–Co–P1, 103.09(4); ∠ CoP1P1'/Co(centC1C2)(centC1'C2') = 28.0(3)º.

In FC$_6$H$_5$ solution **[Co(L1)–NBD][BAr$^F_4$]** reacts quantitatively with H$_2$ to form (in 90% isolated yield) the brown, crystallographically characterized,[21] arene adduct **[Co(L1)(η–FC$_6$H$_5$)][BAr$^F_4$]**, with the concomitant formation of norbornane. This result shows that these cationic Co(I)–systems will promote the hydrogenation of alkenes,[25] similar to the DuPhos variants.[22] For **[Co(L2)–NBD][BAr$^F_4$]** hydrogenation in FC$_6$H$_5$ solution results in decomposition to a mixture of products. However, as we,[12, 26] and others,[27] have previously reported, organometallic synthesis in the solid–state can promote desirable changes in selectivity. This is the case for **[Co(L2)–NBD][BAr$^F_4$]**.

Addition of H$_2$ to single–crystals of **[Co(L2)–NBD][BAr$^F_4$]** results in the formation of the highly reactive σ–alkane complex **[Co(L2)–NBA][BAr$^F_4$]** in a SC–SC transformation. By optimizing H$_2$ addition time (2 bar, 1 hr, 298 K), data collection parameters (2 hrs, –173ºC, frozen oil–drop), and rapid transfer to the diffractometer, an acceptable refinement (R1 = 8%) and unambiguous structural solution was achieved. **[Co(L2)–NBA][BAr$^F_4$]** is so reactive that even at –173 ºC longer data acquisition times than 2 hrs resulted in steady decomposition, loss of diffraction and a color change of the crystal from brown to blue [i.e. Co(II)], which we suggest is due to reaction with adventitious oxygen in the mounting oil.
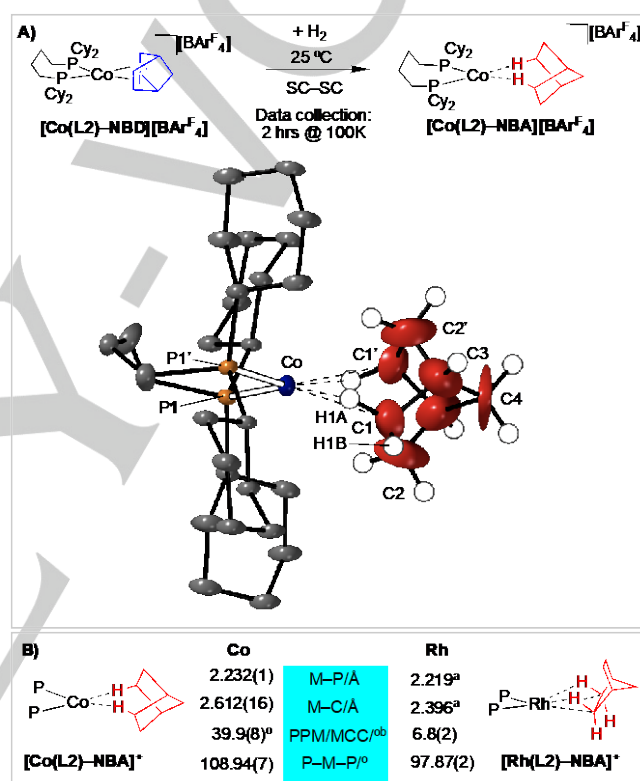

Figure 3. (A) Solid–state structure of the cation in **[Co(L2)–NBA][BAr$^F_4$]**, 15% displacement ellipsoids, anion and most H–atoms not shown. Hydrogen atoms were placed in calculated positions. –173 ºC data collection. Selected bond lengths (Å) and angles (º): Co–P, 2.232(1); Co–C1, 2.612(16); C1–C2, 1.470(12), P1–Co–P1', 108.94(7); ∠ CoP1P1'/CoC1C1' = 39.9(8)º. **(B)** Comparison of selected structural metrics between **[Co(L2)–NBA][BAr$^F_4$]** and **[Rh(L4)–NBA][BAr$^F_4$]**. [a] average distances, [b] angle between planes.

The solid–state structure of **[Co(L2)–NBA]$^+$** is presented in Fig. 3A. This shows a {Co(Cy$_2$P(CH$_2$)$_4$PCy$_2$)$^+$ fragment, with crystallographically–imposed C$_2$ symmetry. The phosphine backbone is disordered over two conformations, and only one is shown.[21] Hydrogen atoms were placed in calculated positions. The metal center is weakly bound with a saturated NBA fragment through two, mutually opposing, endo–Co···H–C interactions: Co···H(1), 1.766 Å; Co···C1, 2.612(16) Å. The other carbon atoms in the NBA ligand are significantly further away [Co···C2, 2.92(2) Å]. The Co–P distances become slightly shorter on hydrogenation

[2.232(1) Å cf. 2.2747(9)], suggesting a weaker *trans*–ligand. As for the precursor, the NBA fragment is twisted away from square planar [∠CoP1P1'/CoC1C1' ~ 40º], see Fig. S12.[21] Overall this is different from the orientation found in **[Rh(L2)–NBA][BAr$^F_4$]** (Fig. 3B), in which the alkane interacts through two adjacent η^2–*endo*–Rh···H–C bonds at a pseudo square planar Rh(I) center. The M···C distances are also ~0.22 Å longer than in **[Rh(L2)–NBA][BAr$^F_4$]**, which is a significant observation given the small difference in covalent radii between Rh(I) and high–spin Co(I) [1.42 and 1.50 Å respectively].[28] While the atomic displacement parameters associated with the Co, phosphine and anion are unremarkable, those of the NBA fragment are both significantly larger and show pronounced ellipticity. This signals the alkane is, relatively, less constrained in the ~ O_h [BAr$^F_4$]$^-$ microenvironment. As a consequence of this the C1–C2 distance in the NBA fragment was restrained to be in the range of a C–C bond, 1.470(12) Å. All these data point to a very weakly bound σ–alkane ligand at a Co(I)–center that is electronically very different from its Rh–analog. That this is a weak intermolecular interaction is signaled by the Co···C distances being much longer than found for the small number of structurally characterized Co···H–C intramolecular agostic complexes [~ 2.2 Å],[29] being more comparable to weak agostic M···H–C interactions [M = Rh, Ir, ~2.8 Å].[30] While rare, σ–alkane complexes of 3d metals have been characterized at low temperature by in situ NMR spectroscopy.[31]

The SC–SC hydrogenation on addition of H$_2$ to **[Co(L2)–NBD][BAr$^F_4$]** is confirmed by adding CD$_2$Cl$_2$ to **[Co(L2)–NBA][BAr$^F_4$]** and vacuum transfer of the volatiles. This shows NBA has been formed (^{1}H NMR), with no residual NBD observed. Addition of H$_2$ to **[Co(L1)–NBD][BAr$^F_4$]** resulted in complete loss of crystallinity, although NBA is – again – formed.
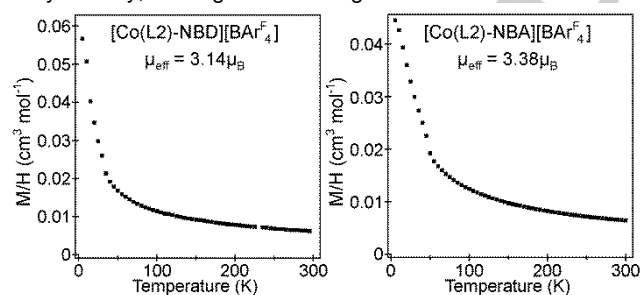

Figure 4. Magnetisation data for **[Co(L2)–NBD][BAr$^F_4$]** and **[Co(L2)–NBA][BAr$^F_4$]**. See supporting materials for more details.

The magnetisation data for both **[Co(L2)–NBD][BAr$^F_4$]** and **[Co(L2)–NBA][BAr$^F_4$]** can be fit by the Curie-Weiss law (χ = C/(T-θ) + K) over the temperature range 50 ≤ T/K ≤ 300 to yield values consistent with a ^{3}Co spin state, Figs. 4 and S14. Low-temperature deviations from Curie-Weiss behavior below 50 K are attributed to intermolecular magnetic couplings. The observation of a temperature independent component to the susceptibility of both compounds is indicative of a small unquenched orbital contribution to the magnetisation, and is consistent with the slightly elevated moments for both compounds,

compared to expected spin-only values: **[Co(L2)–NBD][BAr$^F_4$]** μ$_{eff}$ = 3.14 μ$_B$; **[Co(L2)–NBA][BAr$^F_4$]** μ$_{eff}$ = 3.38 μ$_B$; S = 1, spin-only μ$_{eff}$ = 2.82μ$_B$). The slightly larger moment for the alkane complex is in line with NBA being a weaker field ligand than NBD. Consistent with the ^{3}Co spin state for both complexes ^{31}P{^{1}H} SSNMR spectra are featureless, as are the EPR spectra.

Spin-state energetics for **[Co(L2)–NBA][BAr$^F_4$]** and **[Co(L2)–NBD][BAr$^F_4$]** were also probed with periodic DFT, with geometries based on the crystal structures with H and F positions optimised in the triplet state with the PBE-D3 functional and energies recomputed with the hybrid PBE0-D3 approach.[32] For **[Co(L2)–NBA][BAr$^F_4$]** the ^{3}Co spin-state is favored by 32.3 kcal/mol (at each Co center), consistent with the experimental magnetisation data. In contrast for **[Co(L2)–NBD][BAr$^F_4$]** the ^{3}Co spin-state is only lower by 4.1 kcal/mol and further tests showed the computed preferred spin-state is highly sensitive to both methodology and NBD ligand orientation.[21]

The computed structure of the **[Co(L2)–NBA]$^+$** cation (Fig. 5A) reveals a short Co···H11 distance of 1.82 Å, with an elongation of the C1–H11 bond to 1.12 Å, that together suggest a degree of C1–H11→Co σ–interaction. In contrast, the Co···H21 distance is 2.58 Å and no elongation of the C2–H21 bond is seen. The QTAIM molecular graph (Fig. 5B) is consistent with these features and confirms a Co···H11 bond path. Fig. 5C and D show the NCI plot of the **[Co(L2)–NBA][BAr$^F_4$]** ion-pair, with weak interactions color-coded from blue (most stabilizing), through green (weakly stabilizing) to red (destabilizing). Viewed from the Co centre (Fig. 4C), the localised blue regions between Co···H11 and Co···H11' suggest two η^1-C–H→Co σ-interactions, with turquoise regions between Co···H21/H21' reflecting weaker, dispersive stabilizations. The side-on view of the ion-pair (Fig. 5D) highlights broad regions of dispersive stabilization between the NBA ligand and (i) the PCy$_2$ substituents, (ii) the aryl groups of the [BAr$^F_4$]$^-$ anion and (iii) non-classical C-F···H-C H-bonding, that all serve to stabilize the NBA ligand in the binding pocket.
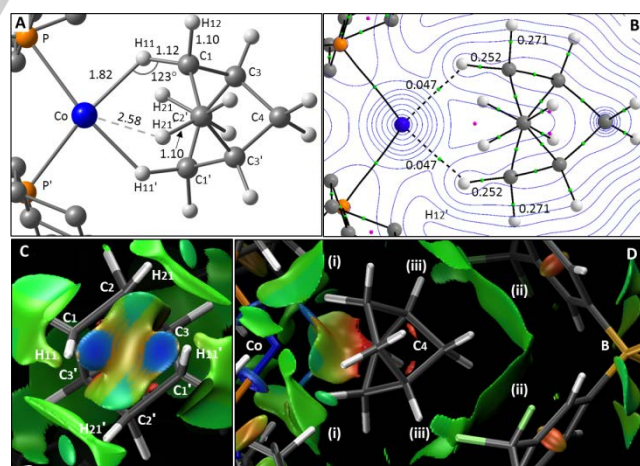

Figure 5. (A) Computed structure of the **[Co(L2)–NBA]$^+$** cation viewed down the C2···C2' axis highlighting key distances (Å) and angles to H atoms. **(B)** Quantum Theory of Atoms in Molecules (QTAIM) molecular graph with bond critical bonds (BCPs) in green, ring critical points (RCPs) in pink and selected BCP electron densities, ρ(r), in eA^{-3}. **(C)** Non-Covalent Interaction (NCI) plot of the proximate **[Co(L2)–NBA][BAr$^F_4$]** ion-pair viewed from the Co center. **(D)**

NCI plot perpendicular to the Co⋯C4⋯B axis highlighting the (i) the PCy$_2$ substituents, (ii) [BAr$^F_4$]⁻ aryl groups, (iii) C-F⋯H-C H-bonding.

A spin-unrestricted NBO 2nd order perturbation analysis delineates interactions in the α- and β–spins at the ^{3}Co center (see Fig. 6, which also gives the Lewis structure used). For α-spin, occupation of all five 3d orbitals means donation from σ$_{C-H}$ can only occur into a Co low-valent (4s) NBO (3.5 kcal/mol). A similar interaction is seen in the β-spin (4.7 kcal/mol), but donation can now also occur into a vacant Co d orbital (5.9 kcal/mol). Back-donation from P lone pairs into the σ*$_{C-H}$ NBOs is seen for both spins, with additional back donation from an occupied Co 3d NBO in the α-spin (1.7 kcal/mol).[21]
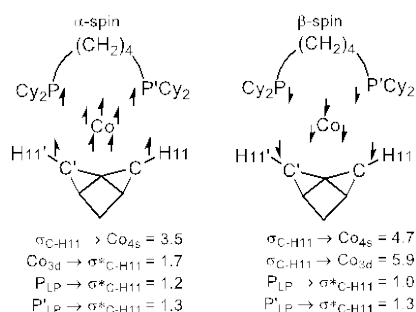

Figure 6. (A) Spin unrestricted NBO 2nd order perturbation analysis highlighting key donor-acceptor interactions (kcal/mol) in **[Co(L2)–NBA]⁺**.

These NBO data indicate NBA is less strongly bound in **[Co(L2)–NBA]⁺** than in the **[Rh(L2)–NBA]⁺** cation (where total σ$_{C-H}$ donation ≈ 19.7 kcal/mol and back-donation to σ*$_{C-H}$ ≈ 8.5 kcal/mol[10]). This also aligns with the reduced C–H11 bond elongation and BCP ρ(r) of the ^{3}Co system. The Co–H11--C angle of 123° along with the localised, stabilizing, features along the C–H11/C'–H11'⋯Co vectors in the NCI plot suggest an η^1:η^1–NBA binding mode in **[Co(L2)–NBA]⁺**, again in contrast with the η^2:η^2–NBA ligand in **[Rh(L2)–NBA]⁺**.[10] The NCI plot also reveals intermolecular dispersive interactions in this ^{3}Co system and these are likely to contribute more to overall stability than in the related, more strongly covalently bound, ^{1}Rh system.

The synthesis of **[Co(L2)–NBA][BAr$^F_4$]** thus rests upon the stabilizing microenvironment provided by the [BAr$^F_4$]⁻ anions, underscoring the importance of such weak interactions in isolating σ–alkane complexes in the solid–state.[3, 9] That this now also allows for the isolation of complexes that sit on a triplet–surface opens up new opportunities for exploring the synthesis, reactivity and catalysis of such species that have, at best, only a fleeting existence when generated in solution.[1, 19]

Conflict of interest

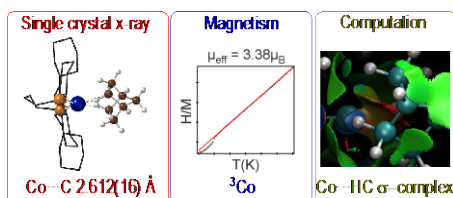The authors declare no conflict of interest.

Acknowledgements

References

[1] C. Hall, R. N. Perutz, *Chem. Rev.* **1996**, *96*, 3125-3146.
[2] R. G. Bergman, *Nature* **2007**, *446*, 391; K. I. Goldberg, A. S. Goldman, *Acc. Chem. Res.* **2017**, *50*, 620-626.
[3] A. S. Weller, F. M. Chadwick, A. I. McKay, in *Adv. Organometallic Chem., Vol. 66* (Ed.: P. J. Pérez), Academic Press, **2016**, pp. 223-276.
[4] S. Geftakis, G. E. Ball, *J. Am. Chem. Soc.* **1998**, *120*, 9953-9954.
[5] W. H. Bernskoetter, C. K. Schauer, K. I. Goldberg, M. Brookhart, *Science* **2009**, *326*, 553.
[6] S. A. Bartlett, N. A. Besley, A. J. Dent, S. Diaz-Moreno, J. Evans, M. L. Hamilton, M. W. D. Hanson-Heine, R. Horvath, V. Manici, X.-Z. Sun, M. Towrie, L. Wu, X. Zhang, M. W. George, *J. Am. Chem. Soc.* **2019**, *141*, 11471-11480.
[7] R. H. Schultz, A. A. Bengali, M. J. Tauber, B. H. Weiller, E. P. Wasserman, K. R. Kyle, C. B. Moore, R. G. Bergman, *J. Am. Chem. Soc.* **1994**, *116*, 7369-7377.
[8] A. L. Pitts, A. Wriglesworth, X.-Z. Sun, J. A. Calladine, S. D. Zarić, M. W. George, M. B. Hall, *J. Am. Chem. Soc.* **2014**, *136*, 8614-8625.
[9] A. J. Martínez-Martínez, B. E. Tegner, A. I. McKay, A. J. Bukvic, N. H. Rees, G. J. Tizzard, S. J. Coles, M. R. Warren, S. A. Macgregor, A. S. Weller, *J. Am. Chem. Soc.* **2018**, *140*, 14958-14970.
[10] A. I. McKay, A. J. Bukvic, B. E. Tegner, A. L. Burnage, A. J. Martínez-Martínez, N. H. Rees, S. A. Macgregor, A. S. Weller, *J. Am. Chem. Soc.* **2019**, *141*, 11700-11712.
[11] S. D. Pike, F. M. Chadwick, N. H. Rees, M. P. Scott, A. S. Weller, T. Krämer, S. A. Macgregor, *J. Am. Chem. Soc.* **2015**, *137*, 820-833.
[12] F. M. Chadwick, A. I. McKay, A. J. Martinez-Martinez, N. H. Rees, T. Krämer, S. A. Macgregor, A. S. Weller, *Chem. Sci.* **2017**, *8*, 6014-6029.
[13] F. M. Chadwick, T. Krämer, T. Gutmann, N. H. Rees, A. L. Thompson, A. J. Edwards, G. Buntkowsky, S. A. Macgregor, A. S. Weller, *J. Am. Chem. Soc.* **2016**, *138*, 13369-13378.
[14] M. D. Walter, P. S. White, C. K. Schauer, M. Brookhart, *J. Am. Chem. Soc.* **2013**, *135*, 15933-15947.
[15] W. E. Billups, S. C. Chang, R. H. Hauge, J. L. Margrave, *J. Am. Chem. Soc.* **1993**, *115*, 2039-2041.
[16] A. A. Bengali, R. G. Bergman, C. B. Moore, *J. Am. Chem. Soc.* **1995**, *117*, 3879-3880; J. P. Lomont, S. C. Nguyen, J. P. Schlegel, M. C. Zoerb, A. D. Hill, C. B. Harris, *J. Am. Chem. Soc.* **2012**, *134*, 3120-3126.
[17] J.-L. Carreón-Macedo, J. N. Harvey, *J. Am. Chem. Soc.* **2004**, *126*, 5789-5797.
[18] T. J. Hebden, A. J. St. John, D. G. Gusev, W. Kaminsky, K. I. Goldberg, D. M. Heinekey, *Angew. Chem. Int. Ed.* **2011**, *50*, 1873-1876; D. L. M. Suess, C. Tsay, J. C. Peters, *J. Am. Chem. Soc.* **2012**, *134*, 14158-14164; K. Tokmic, C. R. Markus, L. Zhu, A. R. Fout, *J. Am. Chem. Soc.* **2016**, *138*, 11907-11913.
[19] X. Wu, Z. Liu, T. S. Murphy, X. Z. Sun, M. W. D. Hanson-Heine, M. Towrie, J. N. Harvey, M. W. George, *Faraday Discussions* **2019**, *DOI: 10.1039/C9FD00067D*.
[20] R. R. Schrock, J. A. Osborn, *J. Am. Chem. Soc.* **1976**, *98*, 4450-4455.
[21] See Supporting Materials for full details
[22] H. Zhong, M. R. Friedfeld, P. J. Chirik, *Angew. Chem. Int. Ed.* **2019**, *58*, 9194-9198.
[23] G. Großheimann, S. Holle, P. W. Jolly, *J. Organomet. Chem.* **1998**, *568*, 205-211.
[24] Z. Freixa, P. W. N. M. van Leeuwen, *Dalton Trans.* **2003**, 1890-1901.
[25] **[Co(L1)–NBD][BAr$^F_4$]** also promotes the catalytic hydrogenation of NBD to NBE and then more slowly to NBD (0.2 mol%, 60 ºC, THF, 12 hours, 1 bar H$_2$)
[26] A. B. Chaplin, J. C. Green, A. S. Weller, *J. Am. Chem. Soc.* **2011**, *133*, 13162-13168.
[27] W. Weng, C. Guo, C. Moura, L. Yang, B. M. Foxman, O. V. Ozerov, *Organometallics* **2005**, *24*, 3487-3499.
[28] B. Cordero, V. Gómez, A. E. Platero-Prats, M. Revés, J. Echeverría, E. Cremades, F. Barragán, S. Alvarez, *Dalton Trans.* **2008**, 2832-2838.
[29] S. Murugesan, B. Stöger, E. Pittenauer, G. Allmaier, L. F. Veiros, K. Kirchner, *Angew. Chem. Int. Ed.* **2016**, *55*, 3045-3048.
[30] R. C. Knighton, J. Emerson-King, J. P. Rourke, C. A. Ohlin, A. B. Chaplin, *Chem. Eur. J.* **2018**, *24*, 4927-4938.

[31] J. A. Calladine, S. B. Duckett, M. W. George, S. L. Matthews, R. N. Perutz, O. Torres, K. Q. Vuong, *J. Am. Chem. Soc.* **2011**, *133*, 2303-2310; O. Torres, J. A. Calladine, S. B. Duckett, M. W. George, R. N. Perutz, *Chem. Sci.* **2015**, *6*, 418-424.

[32] For **[Co(L2)-NBA][BAr$^F_4$]** the disordered phosphine backbone was optimised with local C_2-symmetry

COMMUNICATION

Timothy Morgan Boyd, Bengt E. Tegner, Graham J. Tizzard, Antonio Martínez– Martínez, Samuel E. Neale, Michael A. Hayward, Simon J. Coles, Stuart A. Macgregor,* Andrew S. Weller.*

A Structurally Characterized Cobalt(I) σ– Alkane Complex.

The synthesis, and single–crystal x-ray structure, of a ^{3}Co σ–alkane complex is achieved by a single–crystal to single–crystal solid/gas hydrogenation from a corresponding ^{3}Co–diene precursor.